An Algorithm to Evaluate and Build Schedules for a Distributed Sensor System with Respect to Clock Synchronization

Andreas Puhm, Michael Kramer, and Martin Horauer

University of Applied Sciences Technikum Wien, Vienna, Austria
Email: {andreas.puhm, michael.kramer, martin.horauer}@technikum-wien.at

***Abstract*—Distributed embedded systems utilizing active sensors that share a common media (e.g., light detection and ranging sensors, LIDAR) have to be coordinated to eliminate or reduce interferences between the different sensor nodes. For LIDAR and similar sensor systems it is possible to apply media access methods, like frequency, code and time division multiple access (FDMA, CDMA or TDMA). FDMA and CDMA methods utilize sensor specific parameters for medium access. This can be a drawback, as it is no longer possible or far more difficult to use error correction or measurement enhancement techniques, like multi-frequency measurements, that depend on these parameters. A TDMA scheme frees these sensor specific parameters, but needs additional infrastructure in the form of clock synchronization. The implementation of the synchronization mechanism constrains the TDMA schedules that can be executed. This paper provides an algorithm to ascertain these constraints, and thus determine the requirements for the synchronization mechanism implementation.**

Keywords–Distributed Sensor Network; Clock Synchronization; TDMA; LIDAR.

I. INTRODUCTION

With the advance of distributed sensor systems the need for coordination in such systems arises. Tightly coupled distributed sensor systems need to be coordinated to eliminate measurement errors and correlate results from the individual sensor nodes. For example, if active sensors (e.g., LIDAR or ultrasonic based) are deployed in vicinity, the correct management of the sensor activation and measurement times is a central issue. For applications, like factory automation or indoor positioning, the sensors might be mounted on mobile units. Therefore, simple coordination schemes, like wired triggers, are no longer feasible.

For example, Time-of-Flight (ToF) sensors [1] are available that combine a LIDAR measurement mechanism with a charge-coupled device image sensor. ToF sensors generate image (frame) data similar to a charge-coupled device sensor where each pixel provides distance data in addition to a (gray scale) image. Such a sensor relies on an infrared or laser light source that is activated for each measurement for a certain time. To avoid interference no other light source with the same modulation pattern, e.g., same frequency, should be active during this time. Standard media access schemes, like, FDMA [2], CDMA [3], or phase hopping [4] have been applied to ToF sensor systems. These schemes use different frequencies and/or modulation patterns to eliminate or reduce the interferences between multiple ToF sensors. For a ToF sensor the maximum measurable distance and resolution is determined by the frequency of the light source. Therefore, a media access scheme that utilizes the light source modulation itself, will constrain the sensor with regard to the measurable distance and resolution.

By employing a TDMA scheme, these sensor parameters can be freely used for measurement enhancement processes and error corrections (e.g., [5] and [6]).

Ultrasonic sensors are another type of active sensor, that can be applied for position measurement in a distributed sensor system, e.g., Constellation [7], BUZZ [8], or Cricket [9]. These systems are based on Time-of-Arrival measurements. A radio signal and an ultrasonic signal are generated at the same time by a sending node. The difference of the reception time of these two signals is measured and used to calculate the distance between sender and receiver. In the above mentioned positioning systems multiple beacons are used so that a mobile device can determine the position by correlating the reception time differences. If transmissions of multiple beacons overlap, the measurement results can be erroneous, as a wrong radio signal to ultrasonic signal match can occur. Therefore, they have to be detected and filtered as explained by [9](p.p. 67) or avoided altogether by coordinating the sensors.

Wired triggers (Synchronous BUZZ), radio signals from a central unit (Constellation) or random signal generation on each sender (Asynchronous BUZZ and Cricket) are typically used to coordinate these sensors. In case of wired triggers, the drawback is the need for additional infrastructure (the trigger wires) and the constrained flexibility of such a system (i.e., this is not feasible for mobile sensors). In case of the randomization, the interferences are reduced but not removed. This reduction can be good enough for a small amount of active transmitters in the system but will fall short for larger systems. Even though the synchronization of the measurements via a radio signal solves these problems, it still shares the same weakness: the interoperability with similar systems that are outside of the control of this scheme.

Similar to the ToF sensors, as explained above, various media access schemes from the field of telecommunication have been evaluated and applied for ultrasonic based sensor systems. For example, the Dolphin system [10] uses a direct sequence code division multiple access (DS/CDMA) scheme for measurement coordination of ultrasonic sensors. [11] compare DS/CDMA and frequency hopping spread spectrum (FHSS) media access schemes for ultrasonic sensors and come to the conclusion that FHSS provides a higher accuracy of the measurement results in comparison to DS/CDMA.

Beside ultrasonic sensors, indoor location measurements are also realized by evaluating the received signal strength

 ISBN: 978-1-61208-425-1

indicators (RSSI). [12] describes a location measurement based on RSSI of IEEE 802.15.4 communication beacon messages. Lau et al. find that interferences from IEEE 802.11 traffic operating in the same frequency band cause a high degradation of the precision of the localization measurement due to lost IEEE 802.15.4 beacon messages. A solution for this problem is the scheduling of exclusive time slots for each network protocol.

Media access schemes are abundantly used in the field of telecommunication but can and are also applied to active sensors. Methods that utilize the signal modulation, e.g., CDMA or FDMA, allow the usage of multiple sensors without need for additional infrastructure. The drawback is that these methods either constrain the measurements (FDMA in case of ToF sensors) or do only reduce the interferences (CDMA or random signal activation, e.g., asynchronous BUZZ). Wired triggers, as central coordination method, limit the application scenarios of the system (e.g., it is harder to support mobile units). Using a centrally generated radio signal as trigger source can be a feasible solution, as long as all sensors are in range of the radio signal. If the measurement triggers cannot be derived directly from a central source a distributed clock synchronization is necessary to execute a TDMA schedule. This can be provided by a higher level clock synchronization protocol (e.g., IEEE 1588 or the network time protocol NTP) or is part of the communication network itself (e.g., EtherCAT or FlexRay). The constraints that are added to the system by the clock synchronization and methods to incorporate these in the schedule planning are explained and proposed in this paper.

A distributed system of four Time-of-Flight sensors is presented in Section III. This section introduces the setup of the sensor system, gives a short overview of the ToF sensor principle and derives an ideal TDMA schedule based on the core parameters of the system. Section IV defines the constraints imposed by the clock synchronization on a TDMA schedule. Section IV-E proposes an algorithm set that can be used to calculate these constraints and build an interference-free TDMA schedule that satisfies these constraints. A TDMA schedule in accordance with the calculated upper bound for the synchronization constraints and a supervisor for the synchronization precision have been implemented in the presented system and are described in Section V.

II. Building a Schedule for a Distributed Sensor System

In a system that incorporates multiple active sensors it is necessary to control measurements to reduce or eliminate interference. The term active sensors refers to sensors that generate a signal to execute their measurements (e.g., ToF or ultrasonic sensors). These sensors are typically employed to monitor an object or an area of interest in real time. Therefore, data has to be generated by the sensors at a constant rate f_{meas} and delay between measurements. Thus, a static schedule cycle has to be built. Furthermore it is necessary to calculate the worst case execution time for each measurement T_{wcet} to allocate a time slot in the schedule. The T_{wcet} depends on the sensor type used and is further specified for a Time-of-Flight sensor in the following section. The utilization of the TDMA schedule is the ratio of the allocated time (a sum of all scheduled measurements per time unit) to the available time (e.g., 1 second). In an ideal system it is possible to utilize 100 % of the available time for measurements and to execute the different measurements head-to-head as depicted in Figure 1.

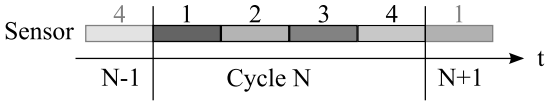

Figure 1: Ideal TDMA Schedule

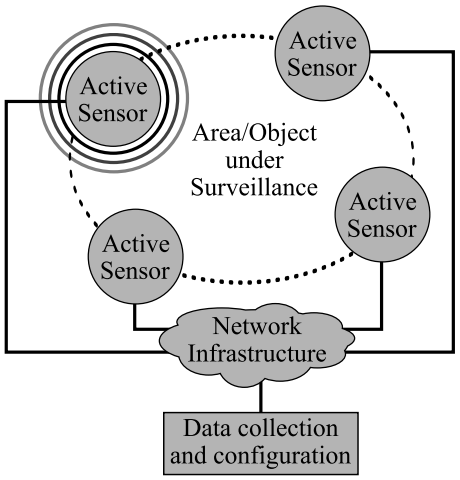

Figure 2: System Overview

III. A Distributed System of ToF Sensors

A system of four ToF sensor nodes of the type Sentis M100 from the company Bluetechnix Group GmbH [13] is used for demonstration as depicted in Figure 2. The sensor measurement configuration is the same for all four sensors. The nodes are connected by 100BASE-TX connections via a switch to a data collector workstation. The workstation is used to calculate the TDMA schedule, configure the trigger modules for each sensor that executes the schedule and to collect measurement data as presented in Section V.

A. Time-of-Flight Sensor Background

A ToF sensor generates a gray scale image of a scene with additional depth information for each pixel. It uses a modulated light source to illuminate the scene. This source is activated for a certain time, also referred to as integration time T_{int}. This typically ranges from 100 μs to 10 ms. After this time of activity of the light source and sensor the gathered data has to be read from the sensor, which takes T_{ro} (in case of the Sentis M100, this is 1.35 ms). During this time another ToF sensor can execute its measurement. However, this is only possible for small integration times ($T_{int} < T_{ro}$). The distance and gray scale data for each pixel can be calculated from a sufficient set of phase measurements N_{phase} (typically 4, [1]). Additional phase measurements can be included for each frame to reduce silicon specific asymmetries of the sensor pixel implementation [1], or to reduce aliasing errors caused by harmonics of the light source [14]. In addition for a worst case measurement time it is necessary to define an upper bound for the integration time, as this parameter can be varied between phase measurements. Therefore, the worst case execution time T_{wcet} for one measurement can be calculated by the sum of the

 ISBN: 978-1-61208-425-1

different phase measurement times defined by the upper bound of the integration time T_{int} for each phase i and the read-out time for the sensor T_{ro} as depicted by (1). In case of the example with the Sentis M100 sensor, each phase measurement has the same integration time and read-out time, and thus, can be simplified to a multiplication of the phase measurement time with the amount of phase measurements N_{phase} as depicted by (2).

$$T_{wcet} = \sum_{i=1}^{N_{phase}} T_{int\_i} + T_{ro} \quad (1)$$

(1) can be simplified in case of the example system:

$$T_{wcet} = N_{phase} \cdot (T_{int} + T_{ro}) \quad (2)$$

B. ToF Sensor System Configuration

For a schedulability analysis the total time T_{sys} that has to be allocated can be calculated by the sum of the measurement times for each sensor in the system. If all (N_{sen}) sensors share the same configuration regarding the measurement time T_{wcet} and the frame rate f_{meas} this can be done by applying (3).

$$T_{sys} = N_{sen} \cdot T_{wcet} \cdot f_{meas} \quad (3)$$

TABLE I: Example system configuration

Parameter	Value	Unit
N_{sen}	4	[1]
f_{meas}	20	$[Hz]$, frames per second
T_{ro}	$1.35 \cdot 10^{-3}$	$[s]$, sensor read-out time
T_{int}	$1.5 \cdot 10^{-3}$	$[s]$, upper bound for the integration time
N_{phase}	4	[1], phase measurements per frame
T_{wcet}	$11.4 \cdot 10^{-3}$	$[s]$, (2) per frame measurement
T_{sys}	0.912	$[s]$, (3) time to be allocated
T_{tot}	1	$[s]$, available time

IV. Synchronization Mechanism Constraints

A. TDMA Schedule Problem

To execute a TDMA schedule in a distributed system a common notion of time is necessary. This is provided by a synchronization mechanism (e.g., IEEE 1588). This mechanism can be characterized by two parameters. The synchronization precision Π and the granularity of the global clock Δ_g. These parameters constrain the resource amount that can be allocated for measurements as depicted by (5), (6), and T_{loss} in Figure 3. In a physical system (Π and Δ_g greater 0 s) it is not possible to execute the TDMA schedule given in Figure 1 without interference between the different tasks.

It is common practice to distribute the spare time evenly between the tasks/measurements. For an interference free execution of measurements it is necessary that the spare time per measurement covers the time loss T_{loss} inflicted by the synchronization mechanism. For the example system the time that has to be allocated is $T_{sys} = 912\ ms$ per second (a utilization of 91.2%).

B. Synchronization Precision

The precision Π_i is the maximum difference of any two clocks of an ensemble at a specific point in time i. The precision of the ensemble (the synchronization precision) Π is the maximum of Π_i over an interval of interest [15, p. 56].

C. Granularity of the Synchronized Global Time

The granularity Δ_g of the global time is the period of the global clock and further the resolution for the triggering of actions (e.g., sensor measurements). Excess time after a scheduled measurement but before the next global clock tick cannot be used for a consecutive measurement.

D. Measurement Time Loss

The synchronization mechanism parameters have to be taken into account for building a TDMA schedule. T_{alloc} (4) depicts the worst case execution time T_{wcet} ((1) or (2)) that has to be allocated per measurement with the addition of the synchronization precision to eliminate interference with consecutive measurements. T_{loss} (5) depicts the loss of measurement time due to synchronization precision and clock granularity for a specific measurement duration. The upper bound for the first term of this equation is Δ_g, and therefore, can be simplified to (6), which depicts the maximum loss per scheduled task in the system.

$$T_{alloc} = T_{wcet} + \Pi \quad (4)$$

$$T_{loss} = \underbrace{\left(\left\lceil \frac{T_{alloc}}{\Delta_g} \right\rceil \cdot \Delta_g\right) - T_{alloc}}_{\leq \Delta_g} + \Pi \quad (5)$$

$$T_{loss}^{max} = \Delta_g + \Pi \quad (6)$$

E. Algorithm Set for the Synchronization Mechanism Constraints

Different synchronization mechanisms and implementation strategies for these mechanisms provide different synchronization precisions and clock granularities. The following algorithm shows how the available slack of a given TDMA schedule can be distributed between these two parameters of the synchronization mechanism.

The time that is not utilized in the TDMA schedule is available as slack S_{tot} (7) and is given by the available time T_{tot} and the necessary time that has to be allocated T_{sys}. By dividing the total slack by the amount of scheduled measurements in the system, the slack budget available per scheduled task S_{task} (8) can be calculated. This can be used to cover the time losses due to the synchronization precision and clock granularity as given by (6).

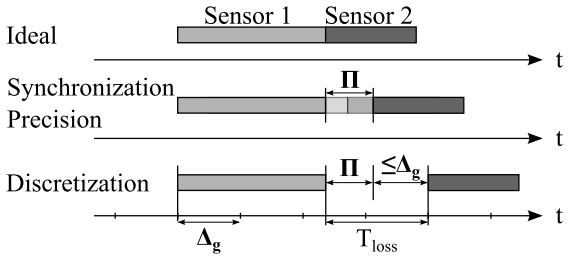

Figure 3: Loss of measurement time due to synchronization precision and clock granularity

$$S_{tot} = T_{tot} - T_{sys} \quad (7)$$

$$S_{task} = \frac{S_{tot}}{\sum_{i=1}^{N_{sen}} f_{meas_i}} \quad (8)$$

$$S_{task} \geq T_{loss}^{max}(6) \quad (9)$$

$$S_{task} \geq \Delta_g + \Pi \quad (10)$$

Therefore, if one of the two parameters is known, the upper bound for the second parameter can be calculated.

F. Applying the Algorithm Set

Starting with the system configuration as given in Table I it is possible to find a set of synchronization parameters that is necessary to execute an interference free TDMA schedule, and therefore, the necessary implementation strategy for the synchronization mechanism. This can be done by setting either the clock granularity or synchronization precision to a fixed value and applying the algorithms defined in Section IV-E to find the corresponding upper bound for the other parameter. The total slack S_{tot} (7) and the available slack per scheduled task S_{task} (8) have to be calculated to solve the inequality (10) for the second synchronization parameter. In case of the example system, (8) can be simplified as all four sensors share the same configuration (f_{meas}).

$$S_{tot} = 1 - 0.912 = 88 \cdot 10^{-3}\ s$$
$$S_{task} = \frac{S_{tot}}{N_{sen} \cdot f_{meas}}$$
$$S_{task} = \frac{88 \cdot 10^{-3}}{4 \cdot 20} = 1.1 \cdot 10^{-3}\ s$$

In case of the example system, the available slack per scheduled task (measurement) is $1.1\ ms$. This can be distributed between the synchronization precision and clock granularity.

Variant 1: Fixed Synchronization Precision

If a legacy system is extended by a synchronization mechanism the type of implementation for this mechanism might be severely constrained. A range for the achievable synchronization precision is given by the type of implementation and the system characteristic (e.g., processor or network load). If the synchronization precision for a system has been measured or estimated it can be used to determine the necessary clock granularity. A software based IEEE 1588 implementation is capable of a synchronization precision Π below $1\ ms$.

$$\text{for} \quad \Pi = 1 \cdot 10^{-3}\ s$$
$$\Delta_g \leq S_{task} - \Pi = 1.1 \cdot 10^{-3} - 1 \cdot 10^{-3} =$$
$$= 0.1 \cdot 10^{-3}\ s$$
$$\Delta_g \leq 100\ \mu s$$

In this case, the clock granularity Δ_g has to be at most $100\ \mu s$ to allow an interference free execution of the TDMA schedule in the example system.

Variant 2: Fixed Clock Granularity

Implementing a fine clock granularity might not be feasible for a system where processor execution time is in high demand. For example, a ToF sensor needs a high amount of execution time for processing the frame data. If a software based implementation of IEEE 1588 is used, a fine clock granularity would add higher processor load to the system. In case of the example system, a coarse granularity of $500\ \mu s$ has been chosen to reduce the additional processor load and the corresponding upper bound for the second parameter, i.e. the synchronization precision Π, is calculated.

$$\text{for} \quad \Delta_g = 0.5 \cdot 10^{-3}\ s$$
$$\Pi \leq S_{task} - \Delta_g = 1.1 \cdot 10^{-3} - 0.5 \cdot 10^{-3} =$$
$$= 0.6 \cdot 10^{-3}\ s$$
$$\Pi \leq 600\ \mu s$$

A synchronization precision Π of $600\ \mu s$ can be reasonably realized by, e.g., a software based IEEE 1588 implementation. Whereas, a typical NTP implementation can achieve a precision down to a few milliseconds, which would not suffice in this case.

G. Choosing or Tuning the Synchronization Mechanism Implementation

With the calculated bounds for the synchronization mechanism parameters it is possible to choose the necessary type and implementation strategy for the system. For example, an IEEE 1588 clock synchronization has two main implementation strategies. A software and a hardware based implementation. In short, a hardware based approach can deliver a synchronization precision down to a few nanoseconds and typically provides a clock granularity of a few nanoseconds. Whereas a software based approach can deliver a synchronization precision in the range of a few microseconds to a few milliseconds. A software implementation of the clock typically provides a clock granularity in the range of $100\ \mu s$ to $1\ ms$. More information regarding these strategies and the achievable synchronization precisions is given in [16].

V. Supervisor for the Synchronization Precision

By building a TDMA schedule with respect to the clock synchronization constraints it is possible to supervise the system by comparing the current precision with the upper bound used to build the schedule. In the example system a local supervisor has been implemented on each sensor. A software version of IEEE 1588 has been implemented with a clock granularity of $500\ \mu s$. The TDMA schedule for the example system has been built with an upper bound for the synchronization precision of $600\ \mu s$ as calculated in variant 2 of Section IV-F.

The synchronization precision Π_i is the highest offset between two sensors in the system at a specific point in time, as defined in Section IV-B. The local supervisors do not have access to values that are generated outside the sensor. Thus, a local supervisor cannot calculate the actual synchronization precision as access to the offsets of the other sensors is not available. The local supervisor has access to the offset from the master (OFM) of the sensor. As shown in Figure 4, the OFM is symmetric around 0. Thus, it is reasonable to assume

 ISBN: 978-1-61208-425-1

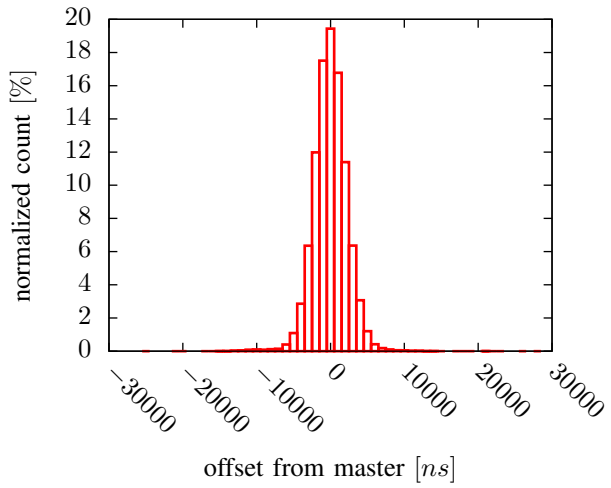

Figure 4: Histogram for the Offset from the Master

that the resulting worst case synchronization precision is two times the worst case OFM and the upper bound for the OFM can be set to $\frac{1}{2}$ of the upper bound for the synchronization precision, i.e. 300 μs. If the OFM rises above this threshold the sensor supervisor disables the measurements for the sensor so that it will not interfere with other sensors.

The synchronization mechanism (in this example IEEE 1588) shares the communication network and the processor execution time with the sensor measurement. Therefore, sensor measurements have an impact on the synchronization mechanism as they need processor time and communication bandwidth.

Three different scenarios have been applied to the system. The internally calculated values for the OFM are transmitted over the communication network and are used offline to calculate the synchronization precision for the system.

Scenario 1: Minimal System Load

In this scenario, no ToF measurements are executed and the communication bandwidth and processor execution time is freely available for the synchronization mechanism. The synchronization precision over the elapsed time (1 hour) is depicted in Figure 5 on the left. A histogram for the synchronization precision is depicted on the right. The average synchronization precision is 3.157 μs and the worst is 28.763 μs.

Scenario 2: Medium System Load

In this scenario, the ToF measurements are executed as given by the system configuration in Section III and the ToF data of two sensors is transmitted over the communication medium. This results in additional load both on the network and the processor side of the system. The measurement results are depicted in Figure 6. The average synchronization precision is 40 μs and the worst is 586 μs, which is below the threshold of 600 μs.

Scenario 3: Full System Load

In this scenario, the ToF measurements are executed as given by the system configuration in Section III and the ToF data of all sensors is transmitted over the communication medium. The measurement results are depicted in Figure 7. The average synchronization precision is 65 μs and the worst is 618 μs, which is above the threshold of 600 μs.

Extrapolation of Scenario 2 and 3

The network load for scenario 3 is twice that from scenario 2. The average synchronization precision rose by 61% from scenario 2 to 3. Additional sensors, and therefore, additional network load will further deteriorate the synchronization precision. Thus, for a system with more than four sensors, either the clock granularity would have to be decreased, or the system slack increased to allow the execution of an interference free TDMA schedule. For the latter, the measurement parameters, i.e. the integration time T_{int} and the frame rate f_{meas}, would have to be reduced.

A. Comparison and Limitations

A non-TDMA based method, as presented by [17], shows a reduction of the impact of interference down to 1.5 % of the maximum measureable distance for a distributed ToF sensor system. In comparison, the TDMA based approach, taking the synchronization mechanism into account as proposed in Section IV-F, shows a standard deviation of the measurement results of 0.07 % of the maximum measureable distance. This is equal to the standard deviation of the measurement of a single sensor. The TDMA approach without a margin for the synchronization parameters, and therefore, a head-to-head scheduling of the sensors, results in a standard deviation of 0.6 %. The worst case scenario for the sensor system is a measurement of all sensors at the same time. This results in an erratic distribution of the measured distance values between 1 % and 1000 % of the actual distance.

By applying a TDMA schedule and the supervisor to the system it is possible to eliminate the interferences between the sensors, if the following points are accounted for:

- The limits for the precision of the synchronization mechanism. These have to be determined correctly (typically offline) to build a valid TDMA schedule by utilizing the proposed algorithm.
- The accuracy of the online synchronization precision measurement. This value will be used by the supervisor to check against the previously (offline) defined limits for the synchronization precision.

It is also necessary to consider how the supervisor has to interact with the system. It can either mark invalid measurements, or disable measurements if the measured precision deteriorates over a certain threshold. Thus, it has to be considered if a missing measurement might actually cause more harm to a system than a measurement with a certain error due to interference.

VI. Conclusion

As it has been shown in Section I, various sensor control methods have been implemented by research groups, ranging from simple central wired or wireless methods to typical media access schemes, like CDMA. The advantages and disadvantages of these methods for active sensors have been discussed. A TDMA scheme provides a control method that is decoupled from the measurement mechanism of active sensors but needs a clock synchronization mechanism in the background and a valid TDMA schedule for operation.

 ISBN: 978-1-61208-425-1

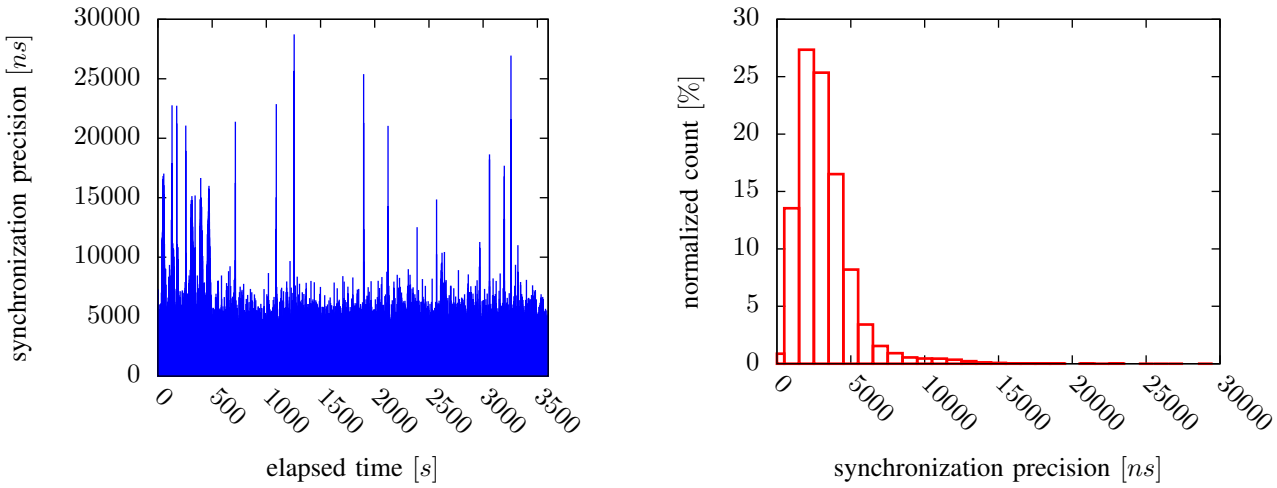

Figure 5: Scenario 1: Minimum System Load

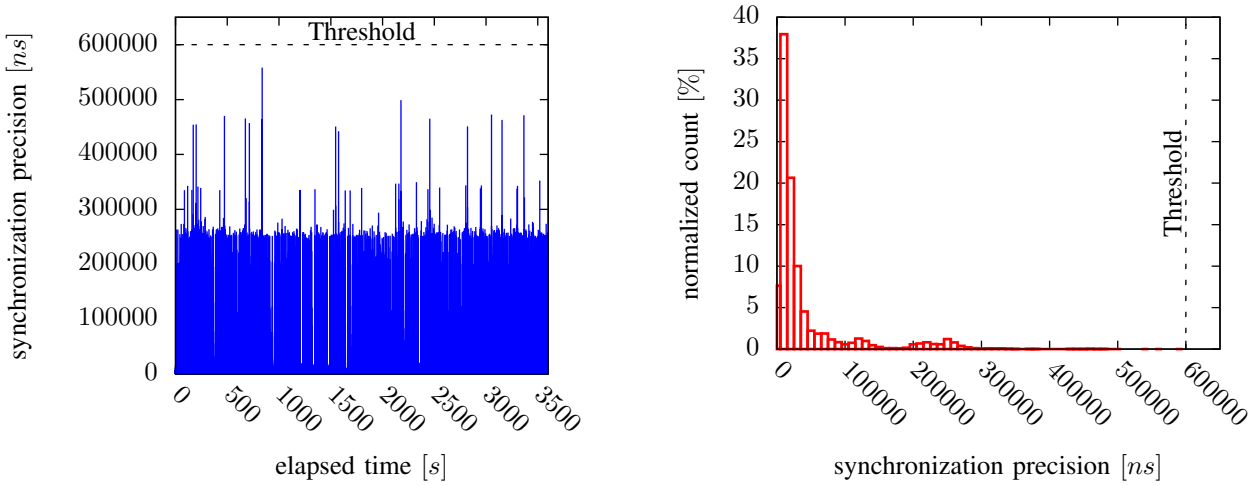

Figure 6: Scenario 2: Medium System Load

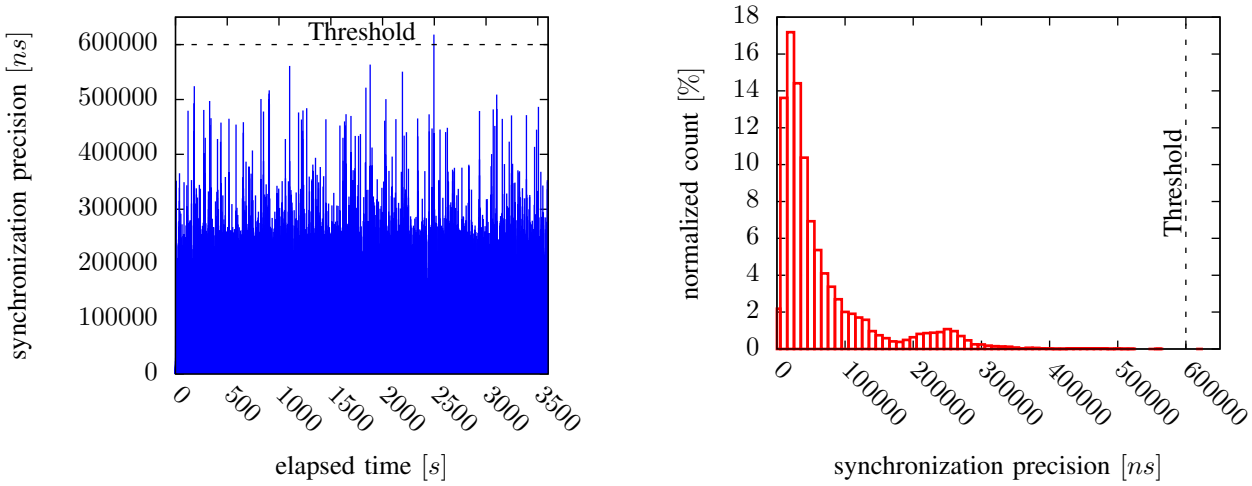

Figure 7: Scenario 3: Full System Load

 ISBN: 978-1-61208-425-1

In Subsection IV-A, it has been shown that not every schedule for a distributed sensor system is feasible if the underlying synchronization mechanism is not taken into account. The imposed synchronization mechanism constraints can be calculated, and thus, incorporated into the schedule planning to deliver a valid and executable TDMA schedule for the system. An algorithm set for this calculation has been proposed in Subsection IV-E.

This algorithm set can be used to set the bounds of the constraints of the synchronization mechanism for the system, especially the synchronization precision. Further, the synchronization precision can be monitored in the system and proper actions can be set, e.g., disabling task executions until the precision is below a specified threshold. This is especially interesting for a system of active sensors, for example, the ToF sensor system described in Section III, where it is necessary to eliminate interference of the scheduled measurements. A simple local supervisor has been implemented in the example system and measurements of the synchronization precision of an IEEE 1588 software implementation for different scenarios have been presented in Section V.

ACKNOWLEDGMENT

This work has been supported by Bluetechnix Group GmbH and by the public funded R&D project Josef Ressel Center for Verification of Embedded Computing Systems (VECS) managed by the CDG.

REFERENCES

[1] R. Kaufmann et al., "A time-of-flight line sensor: development and application," in Proceedings SPIE 5459, Optical Sensing, 2004, pp. 1–8.

[2] C. Bamji. Method and system to avoid inter-system interference for phase-based time-of-flight systems. US Patent 7,405,812. [Online]. Available: http://www.google.com/patents/US7405812 [retrieved: Jun., 2015]

[3] B. Buettgen, M.-A. El Mechat, F. Lustenberger, and P. Seitz, "Pseudonoise optical modulation for real-time 3-d imaging with minimum interference," in Circuits and Systems I: Regular Papers, IEEE Transactions on (Volume:54 , Issue: 10), 2007, pp. 2109–2119.

[4] T. Oggier, B. Buettgen, and M. Schweizer. System and method for multi tof camera operation using phase hopping. US Patent App. 13/280,154. [Online]. Available: https://www.google.com/patents/US20120098964 [retrieved: Jun., 2015]

[5] A. Dorrington, J. Godbaz, M. Cree, A. Payne, and L. Streeter, "Separating true range measurements from multi-path and scattering interference in commercial range cameras," in Proceedings SPIE 7864, Three-Dimensional Imaging, Interaction, and Measurement, 2011, pp. 1–10.

[6] A. Payne, A. Jongenelen, A. Dorrington, M. Cree, and D. Carnegie, "Multiple frequency range imaging to remove measurement ambiguity," in In Proceedings of at 9th Conference on Optical 3-D Measurement Techniques, Vienna, Austria, 2009, pp. 139–148.

[7] E. Foxlin, M. Harrington, and G. Pfeifer, "Constellation: A wide-range wireless motion-tracking system for augmented reality and virtual set applications," in Proc. ACM Conf. on Computer Graphics and Interactive Techniques (SIGGRAPH '98), 1998, pp. 371–378.

[8] M. R. McCarthy, "The buzz: Narrowband ultrasonic positioning for wearable computers," Ph.D. dissertation, University of Bristol, 2007.

[9] N. B. Priyantha, "The cricket indoor location system," Ph.D. dissertation, Massachusetts Institute of Technology, 2005.

[10] M. Hazas and A. Hopper, "Broadband ultrasonic location systems for improved indoor positioning," Mobile Computing, IEEE Transactions on, vol. 5, no. 5, May 2006, pp. 536–547.

[11] J. Gonzalez Hernandez and C. Bleakley, "High-precision robust broadband ultrasonic location and orientation estimation," Selected Topics in Signal Processing, IEEE Journal of, vol. 3, no. 5, Oct 2009, pp. 832–844.

[12] S.-Y. Lau, T.-H. Lin, T.-Y. Huang, I.-H. Ng, and P. Huang, "A measurement study of zigbee-based indoor localization systems under rf interference," in Proceedings of the 4th ACM International Workshop on Experimental Evaluation and Characterization, ser. WINTECH '09. New York, NY, USA: ACM, 2009, pp. 35–42. [Online]. Available: http://doi.acm.org/10.1145/1614293.1614300

[13] Sentis m100 tof smart sensor. internet. Bluetechnix Group GmbH. Http://www.bluetechnix.com/de/products/depthsensing/. [Online]. Available: http://www.bluetechnix.com/de/products/depthsensing/ [retrieved: Jun., 2015]

[14] J. P. Godbaz, M. J. Cree, and A. A. Dorrington, "Understanding and ameliorating non-linear phase and amplitude responses in amcw lidar," Remote Sensing, vol. 4, no. 1, 2011, pp. 21–42.

[15] H. Kopetz, Real-Time Systems, 2nd ed. Springer, 2011.

[16] A. Puhm, M. Kramer, P. Moosbrugger, and M. Horauer, "Problems and solutions for refitting a sensor network with ieee1588 clock synchronisation," in Proceedings of the 19th IEEE International Conference on Emerging Technologies and Factory Automation (ETFA'2014), 2014, pp. 1–7.

[17] B. Buettgen and P. Seitz, "Robust optical time-of-flight range imaging based on smart pixel structures," in Circuits and Systems I: Regular Papers, IEEE Transactions on (Volume:55 , Issue: 6), 2008, pp. 1512–1525.

 ISBN: 978-1-61208-425-1